MONTE CARLO STUDIES OF THE EFFECTS OF PROTEIN, CHOLESTEROL AND CURVATURE ON LIPID ORDER PARAMETERS

By

SHEAU-LIN SHARON CHERNG

Bachelor of Science

National Taiwan Normal University

Taipei, Republic of China

1973

Submitted to the Faculty of the Graduate College
of the Oklahoma State University
in partial fulfillment of the requirements
for the Degree of
MASTER OF SCIENCE
May, 1978

MONTE CARLO STUDIES OF THE EFFECTS OF PROTEIN,

CHOLESTEROL AND CURVATURE ON LIPID

ORDER PARAMETERS

Thesis Approved:

Hugh L. Scott
Thesis Adviser

R. C. Powell

H. Alan Spivey

Norman N Durham
Dean of the Graduate College

ACKNOWLEDGMENTS

The author wishes to express her appreciation to her major adviser, Dr. H. L. Scott, for suggesting this problem and for his patient guidance and encouragement throughout this study. Appreciation is also extended to the members of her committee, Dr. R. C. Powell and Dr. H. O. Spivey, for their help and advice.

TABLE OF CONTENTS

LIST OF FIGURES

CHAPTER I

INTRODUCTION

The purpose of this thesis is to explore the nature of lipid-protein and lipid-cholesterol interactions in biological memberanes through using the Monte-Carlo method. There are many different types of biomembranes and sometimes even one particular biomembrane is composed of several different lipids and proteins. The problem of describing biomembrane structure in terms of how the various lipids and proteins may interact is therefore complicated in real cell membranes, and it is not surprising that many structures have been suggested to describe them. The most commonly accepted model is the "fluid mosaic model" (1). This model is based upon the lipid bilayer. In lipid bilayers two kins of non-covalent interactions are most important, hydrophobic and hydrophilic. Hydrophobic interactions cause non-polar groups (alkyl chains) to move away from water. By hydrophilic interactions we mean the preference of ionic and polar groups for water rather than a non-polar environment. The polar head of lipid molecules at the exterior surface of the bilayer is in direct contact with water, thereby maximizing hydrophilic interaction. Furthermore, the non-polar fatty acid chains or hydrocarbon chains are between the head groups and sequestered together away from contact with water, thereby maximizing hydrophobic interaction. The membrane protein could be disposed

with lipids in three ways: 1) attached to the membrane surface, 2) partially penetrated in lipid bilayers, or 3) penetrating entirely through the biomembrane, as shown in Figure 1. When proteins and cholesterol are incorporated into lipid bilayer, they influence the ordering of the lipid bilayer (2). The fluidity of the lipid bilayer could effect enzyme function in biological membranes (3,4). Thus, knowing how proteins and cholesterol interact with lipids can help us to better understand some of the functions of biological membranes. Lipids and proteins are major components of biomembranes. If we are to understand the structure of biomembranes, we must first understand the structure and interactions of lipids and proteins in bilayers and related structures.

Lipids are amphipathic organic substances, containing both hydrophobic tails and a hydrophilic head group. The hydrophobic and hydrophilic regions can be connected by a glycerol molecule, or a sphingosine molecule, as shown in Figure 2. The lipids vary by different hydrocarbon chainlength or bond saturation, or by polar head group. For example a typical widely studied phospholipid, dipalmitoyl phosphatidylcholine (DPPC), has a glycerol backbone, a phosphate polar head group and two 16:0 saturated hydrocarbon chains, as shown in Figure 2. Sphingomyelin whose polar head group, phosphate and choline, based on the sphingosine molecule, has one 15:1 hydrocarbon chain, while the other one is some saturated fatty acid, as shown in Figure 2 (5).

Lipids have a variety of unusual physical properties. We want to consider their behavior in terms of their ability to form liquid

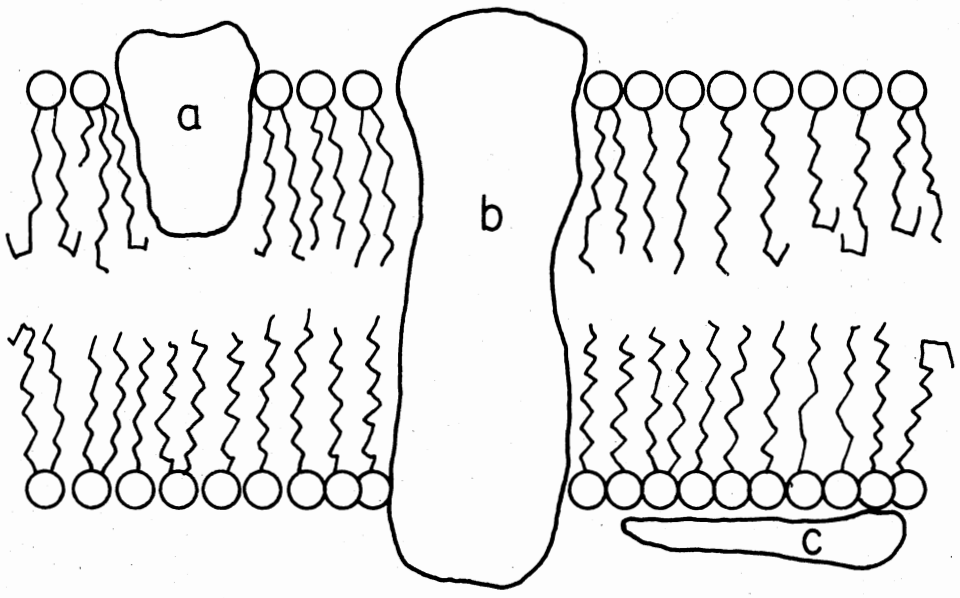

Figure 1. A Schematic Drawing of Structure of Biomembrane. The Circles Represent the Head Groups. The Zig-Zag Lines Represent the Hydrocarbon Chains. The Space Marked a, b, c Represent Proteins Which Penetrate Totally (b) or Partially (a) Through or Simply Contact Externally (c) with Biomembrane

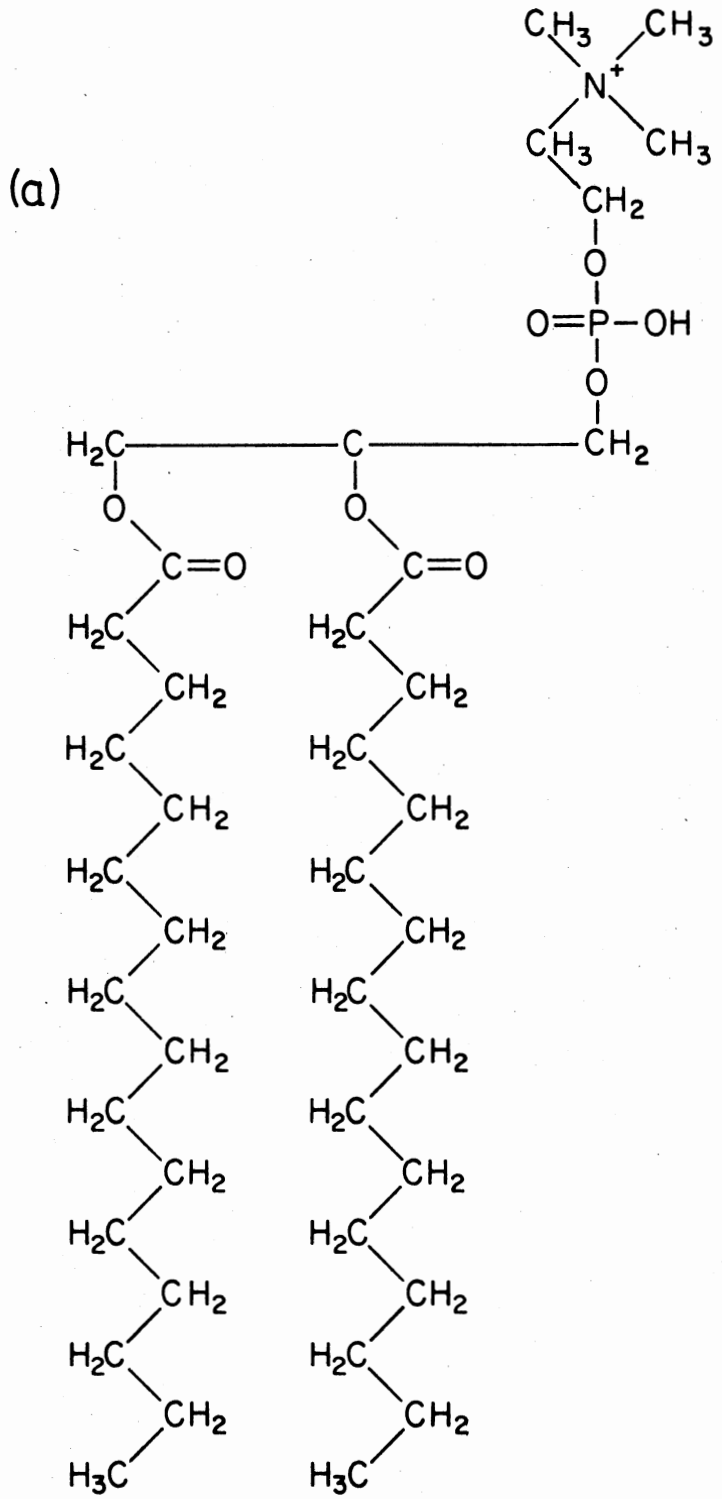

Figure 2. Chemical Structure of a) Dipalmitoyl Phosphatidylcholine (DPPC) and b) Sphingomyelin

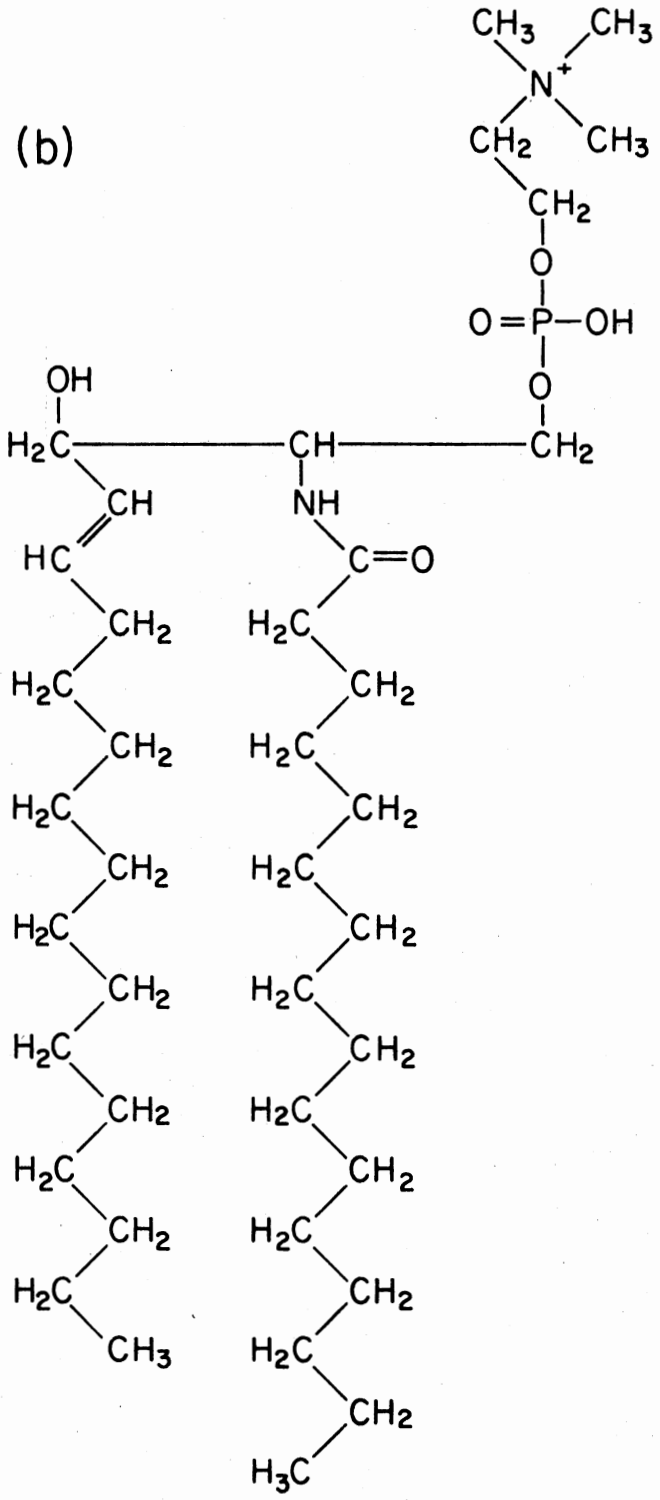

Figure 2. (Continued)

lyotropically. When water is added to phospholipids the resulting structures depend on both temperature and water content. There is a minimum temperature Tc* (Kraft temperature)below which water cannot penetrate into crystal lattice of polar lipids. The phase transition temperature Tc depends upon the nature of the hydrocarbon chains and of the polar region of molecule, the amount of water present. After the water has penetrated into the lattice of phospholipid if the temperature drops below Tc, then the hydrocarbon chains are packed in a crystalline lattice which are separated by excess water layers. If the temperature is above Tc, the hydrocarbon chains are melted and form multi-lamelar phase, as shown in Figure 3.

Phase transition in lipid bilayers have been observed by calorimetry (6), x-ray diffraction (7) and spin label resonance (8) techniques. X-ray studies (7) show that below the transition temperature the hydrocarbon chains produce a sharp diffraction pattern with 4.8 $\mathring{A}$ distance between nearest neighbor chain. Above the transition the diffraction pattern is quite diffuse. Nagle and Wilkinson (9) use differential dilatometer to measure the volume change for dipalmitoyl phosphatidylcholine-water system. The volume of the lipid material increase of about .037 mg/ml is observed at the main transition temperature 41.4^{o}C.

Theoretical interpretation of the experimental results are proposed by several workers (10,11,12,13). They suggested a simple model for hydrocarbon chain order-disorder behavior. There are three states available to each carbon-carbon bond of hydrocarbon chain, one "trans" state and two "gauche" states, as described below. The energy

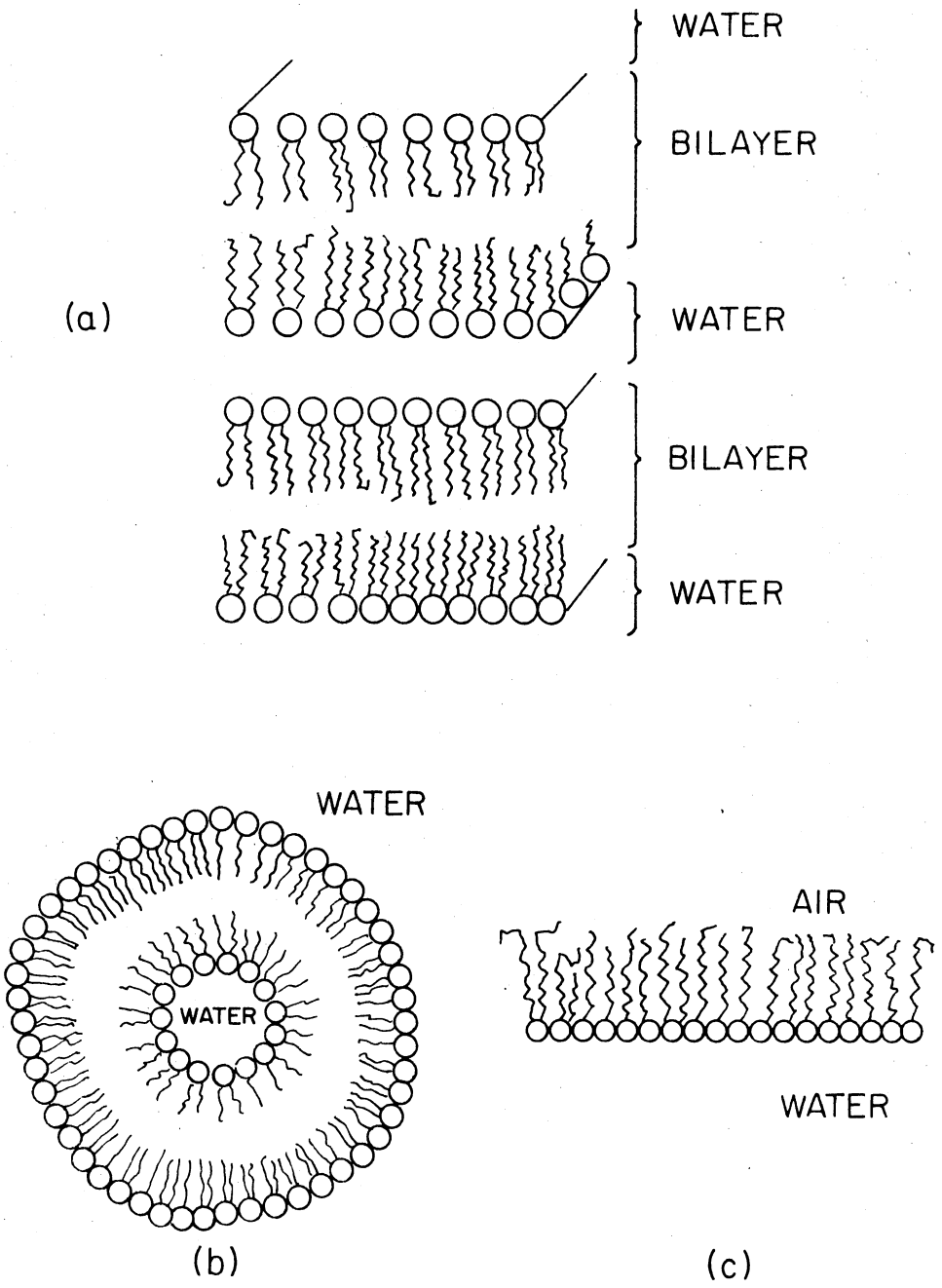

Figure 3. "Model Membranes" for Lipid Dispersed in Water: a) Multi-Lamelar: Sheets of Parallel Lipid Bilayers Separated by Water. b) Vesicles: a Spherical Bilayer Which can be Formed by Using Sonication Upon Multi-Bilayers. c) Monolayer Film Formed at Air-Water Interface

for the formation of a gauche state is 0.5 Kcal/mole higher than at trans state, so that at low temperature the hydrocarbon chains are most likely in the all trans state, as shown in Figure 4. Figure 4 also shows the conformations of gauche rotations. The gauche rotation is formed by rotating about a carbon-carbon bond by an angle of $+120^{o}$ or -120^{o}. As shown in Figure 4, when gauche rotation is formed the length of hydrocarbon chain has shortened compared to the all trans state chain. At physiological temperature there will be some chance that carbon-carbon bond change from trans state to gauche states. However, when carbon-carbon bond rotate the free end of the hydrocarbon chain cannot overlap with another hydrocarbon chain. So usually the single gauche rotation will not happen until the hydrocarbon chains are widely separated. However, cooperative rotations at higher densities do occur during the main transition in pure lipid bilayer (10).

At water concentrations above 40%, then we can use ultrasonication to form bilayer vesicles (liposome). Liposomes are also biomembrane modesl. This kind of model is very useful for studying ion permeability in lipid bilayers.

A monolayer formed at air-water interface, as shown in Figure 3, provides a very useful model membrane system. There are certain advantages to using monolayer model systems. One is that the experimenter can use the parameters A (area per lipid molecule) and π (the lateral pressure). The area per lipid molecule can be easily altered by expanding or compressing the confining area of the surface film, but this process cannot be done easily in the other model system. We can consider monolayers as a model systems for membranes simply

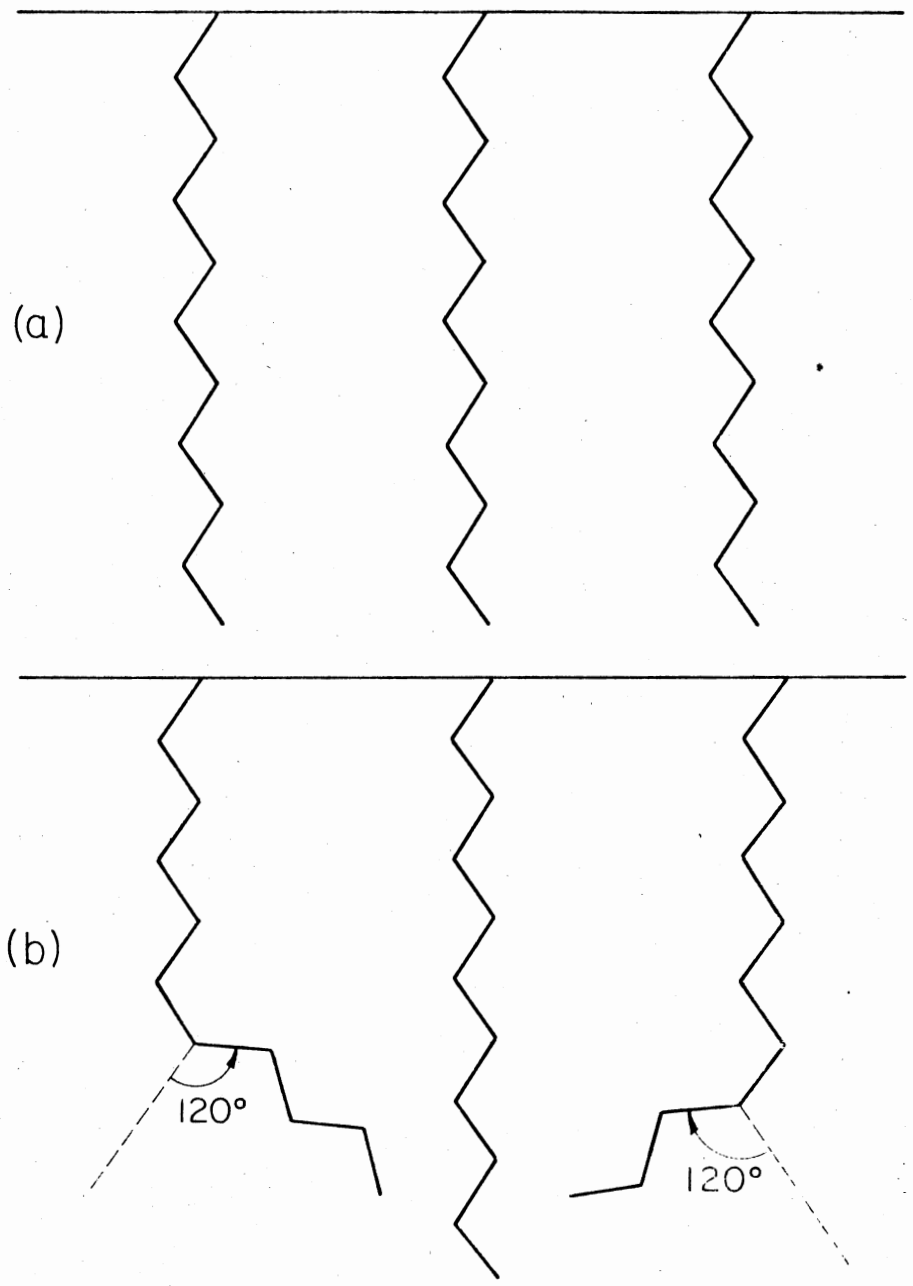

Figure 4. Trans and Gauche Rotational Conformations. a) Trans State Conformation. The Angle Between Bonds is 109.5°. b) Gauche Rotational Conformation. On the Left Side Shows +120° Gauche Rotation. The -120° Gauche Rotation is Shown on the Right Side. The Chain in the Middle is All Trans State Chain for Comparison. After Gauche Rotations the Chain Length is Shorter Than All Trans State Chain

because a bilayer is composed by two monolayers tail to tail with only weak interaction between the two monolayers. Phillips and Chapman (14) using a surface trough suggest that the monolayer critical temperature for DPPC is close to 41^{o}C. This temperature is analogous to the temperature of the major endothermic peak seen by differential scanning calorimetry (41.5^{o}C) with a DPPC bilayer vesicles. So there is some direct correlation between lipid monolayer and bilayer.

Proteins play a wide variety of roles in biomembranes. They can contribute to the structural integrity of the membrane. They can act as enzymes, or they can function as pumps moving material into and out of cells. There are two basic types of membrane proteins, extrinsic and intrinsic, based on their ease of dissociation from the biomembrane. Extrinsic proteins are associated with the polar head groups of the lipid bilayer, such as spectrin and can be easily removed from lipids. Intrinsic protein penetrate partially or totally through the biomembrane. Such protein is presumably in a conformation such that, like Glycophorin, the part in contact with the polar head of lipids and water is hydrophilic and the rest, associated with hydrocarbon chains, is hydrophobic as shown in Figure 1. Usually it is not easy to dissociate the intrinsic proteins from biomembranes.

Biomembranes are hetergeneous mixtures of lipids, cholesterol and proteins, thus it is important to consider that there will be some interactions between them. From understanding the interaction between them we might eventually be able to understand some of the structure-function relationships in biomembrane. A number of experimental studies of lipid-protein and lipid-cholesterol interactions have been

performed using various techniques, e.g., freeze etch fracture (15), x-ray diffraction (16), spin label spectroscopy (17,18) and thermal differential calorimetry (19, 20). Chapman (19) from his differential scanning calorimetry results showed that when lipids of the same class are mixed they did not show a great change in the range of thermal transition. On the other hand when lipids from two different classes (of different chain length) are mixed, a considerable increase in transition range occurs. It is because the transition temperature for the two pure components (lipids) do not coincide. If certain basic proteins (cytochrome C oxidase, lysozme) are incorporated into phosphatidylserine, the gel-liquid crystalline transition temperature shifts down by $7^{o}C$.

Papahadjopoulos et al. (15) use freeze fracture to compare the fracture surface of liposome membranes with and without a hydrophobic protein from human brain myelin. The freeze fracture surface of liposome membrane is not smooth but shows a particulate fractur surface with protein. They claim that the protein has embedded into the liposome bilayer to make the particulate fracture surface. Later they use differential scanning calorimetry (20) to examine the effects of proteins on the permeability of phospholipid vesicles and the expansion of phospholipid mono-molecular film at the air-water interface. They found proteins such as cytochrome C which partially penetrate the bilayer increase both the vesicle permeability to sodium and area per molecule in monolayers. There are not substantial differences when ribonuclease and polylysine, which attach externally on bilayers are incorporated. The $^{22}Na^{+}$ permeability of phospholipid membranes was found to be dependent on the ability of penetration of proteins

(lysozyme, cytochrome C and ribonuclease) into phospholipid membrane (21).

Jost concluded from ESR studies (17,18) that there is a single layer of phospholipid, known as boundary lipid, bound to the hydrophobic protein surface of cytochrome C oxidase. This boundary lipid is rather immobile, while the lipid bilayer beyond the boundary lipid is more fluid. The amount of boundary lipid seems to be relatively constant regardless of the amount of mobile lipids. Marcelja (22) came to the similar conclusion using a theoretical model. He used a molecular field approximation to calculate the order parameter of the annuli of the phospholipid molecules surrounding a protein and found that the most profound perturbation of the phospholipid molecules is the first nearest neighbor molecules. Phase diagrams for the system dimyristoyl phosphatidylcholine-protein have been produced from spin lable studies by McConnell (2) also indicate that there is a layer of immobilized lipid molecules around a protein molecule.

McConnell also determined the phase diagram for dimyristoyl phosphatidylcholine-cholesterol mixtures. From that phase diagram they concluded that two solid phase coexist below 23^{o}C when cholesterol contained from 0% to 20%. At temperatures above 23^{o}C solid and fluid domains coexist. In studies with phospholipid suspensions in water, the addition of cholesterol restricts the motion of the CH_2 groups of the phospholipid hydrocarbon chains. The broadening of protein magnetic resonance spectra (23) and x-ray diffraction (24) studies of phospholipid-cholesterol system indicate that at $T \leq Tc$ incorporated cholesterol produces a smaller surface area per pholpholipid molecule

and increases the thickness of the lipid layer. However, if the temperature of the phospholipid is above the transition temperature, the cholesterol plays a different role, tending to liquify phospholipid. This effect is best observed by differential scanning calorimetry (25) as the disappearance of the endothermic peak due to the phospholipid at the transition temperature and by x-ray diffraction (26) as the appearance of a diffuse high angle spacing at 4.45 Å, instead of a sharp 4.2 Å space.

From the discussions above, we do see abundant evidence of interaction between lipid and protein or lipid and cholesterol. In the following chapter we want to use the Monte Carlo method to consider the effect of protein and cholesterol on lipids. The Monte Carlo simulation we will use is based on a Scott's method (27). In his paper Scott used the Monte Carlo method to simulate the hydrocarbon chains in monolayer and to calculate the order parameters of hydrocarbon chains. For this study we want to extend this technique to calculate the order parameters of hydrocarbon chains after the addition of protein and cholesterol molecules.

So far all the hydrocarbon chains we simulated are confined to a planar monolayer or half a bilayer. As a matter of fact there exist some regions that lipids exhibit spherical bilayer (liposome). Chrezsczyk et al. (28) have used phosphorus-31 NMR to study solutions of small L-α-dipalmitoylphosphatidylcholine (DPL) bilayer vesicles containing sodium dimethyl phosphate and determined the radial length of the DPL inner monolayer (head group portion is narrower than tail region) and outer monolayer (head group portion is wider than tail region). According to their results, the inner monolayer is shorter,

15 Å, so the chains in inner monolayer are more folded. The outer monolayer is thicker, 20 Å, the chains are relatively extended. They suggested that the curvature of bilayer will effect the fluidity and may effect the physical state of biomembrane on its biological function. So as an additional application of the Monte Carlo method we will calculate the order parameter of hydrocarbon chains confined in a curved boundary.

CHAPTER II

THEORY

The term "Monte Carlo" denoted in 1942, at Los Alamos, a secret file concerning studies by John von Neumann. The Monte Carlo method, in all its form, involves the use of random numbers which are generated by a completely deterministic arithmatical process. In Monte Carlo computation, one draws samples from some parent population by using sampling procedures which are governed by specified probabilities. Then collect the statistical data from the samples, and through analysis of these data one will get inferences concerning the parent population. There are two catagories of Monte Carlo methods, analog (direct simulation) and nonanalog. If we simulate phenomena we wish to study by imitating a random sampling in the real world, this Monte Carlo process is an analog process. The nonanalog process originated from von Newmann-Ulam's concept which involves equations solved by constructing by random samplings, an equivalent statistical system. In other words we wish to immerse the given problem into a statistical problem. The ideas behind the analog Monte Carlo method are simple and economical. However, the analog method has serious disadvantages. Suppose that we are interested in studying events which, in a given system, occur only very rarely. These events will also rarely occur in an abstract analog of the system. Vast stores of

data taken from the analog may contain little information which has value for us. Many techniques have been devised to improve the information content in Monte Carlo samples. The importance sampling (29) method is the one we want to use. The importance sampling involves a distortion of the actual physical transition probabilities with the net result that events of interest in the calculation will occur more frequently than in the analog process. This distortion is then compensated by a corresponding alteration of the estimated random variable so as to remove any bias from the estimates of the quantities of interest.

In our studies, we want to evaluate some average quantities such as chain length and chain order parameter (defined later) at statistical equilibrium. In statistics, if we use canonical ensemble the average of an observable quantity F is given by

$$F = \int F \exp(-E/kT)dr \; / \int \exp(-E/kT)dr \qquad (1)$$

where $r = (r_1, r_2, \ldots\ldots r_N)$, with r_i is the position vector of molecule i. E is the total energy of the system.

It is usually impractical to attempt to evaluate these integrals by the usual numerical method. So we resort to Monte Carlo method. The method which we have used is the same as that used by Scott in his Monte Carlo simulation of hydrocarbon chains in a lipid monolayer (27). In this simulation, we begin with a fixed number of chains. The first carbon of each chain is confined to an array in the YZ-plane of specified size. The remainder of the chains lies below the YZ-plane. The positions of the remaining carbon atoms in each chain can be

calculated in the following manner. We define our variables which we will use for the equations.

1. R_i is the displacement vector which show length of each carbon-carbon bond projected on X,Y,Z axis, i represents the bond number.

2. $$R_o t_i = \begin{bmatrix} \text{Cos}\theta & \text{Sin}\theta\text{Cos}\phi_i & \text{Sin}\theta\text{Sin}\phi_i \\ \text{Sin}\theta & -\text{Cos}\theta\text{Cos}\phi_i & -\text{Cos}\theta\text{Sin}\phi_i \\ 0 & -\text{Sin}\phi_i & \text{Cos}\phi_i \end{bmatrix} \quad (2)$$

is the rotation operators matrix. θ is the angle between successive bonds, set at 70.5^o, and ϕ_i is the gauche angle for each bond. The allowed values for ϕ_i in the rotational isomeric approximation are 0^o and $\pm 120^o$, corresponding to states represented by t (trans) and $\pm$ g (gauche $\pm$).

3. $$A_i = (R_o t_1)(R_o t_2).....(R_0 t_i) \quad (3)$$

4. P_j is the matrix which represents the position of every carbon.

5. $$B = \begin{bmatrix} \text{Cos}(\theta/2) & \text{Sin}(\theta/2) & 0 \\ -\text{Sin}(\theta/2)\text{Cos}(RA) & \text{Cos}(\theta/2)\text{Cos}(RA) & \text{Sin}(RA) \\ \text{Sin}(\theta/2)\text{Sin}(RA) & -\text{Cos}(\theta/2)\text{Sin}(RA) & \text{Cos}(RA) \end{bmatrix} \quad (4)$$

where $\theta = 70.5^o$, RA is some small angle, $0 \leq RA \leq 1$, representing a rotation of the entire chain around a central axis. At first step we initialize the chains in the all trans comformation. So we set Cos(RA) = 1. and Sin(RA) = 0.

We set $R_1 = \begin{pmatrix} 1 \\ 0 \\ 0 \end{pmatrix}$ for link 1 of each chain. The remaining links of each chain project on X,Y,Z axis can be generated from multiple application of the rotation operator $R_o t_i$. We write in the form

$$R_{i+1} = A_i R_i \tag{5}$$

Since we started with chains in the all trans state, so ϕ_i at the beginning is 0^o. Now we have the components of each link along the X,Y,Z axis. We want to write them in a coordinated system. But if we now add those components we obtain a chain as shown in Figure 5. The whole chain is $70.5^o/2$ tilted from X-axis. Since we want them perpendicular to YZ-plane, we use B to rotate each link $70.5^o/2$, then use P_j to get the position of every carbon atom. We summarize this in the next equation

$$P_j = P_i + B \cdot R_i \tag{6}$$

$j = 1,2.....i+1.$

Figure 5 shows the aspect of all trans state chain.

After we initialized the chains, we pick a chain at random and translate this chain a random distance less than one half lattice unit (the units are chosen so that the carbon-carbon bond length is unity). Then we randomly choose a bond on the same chain and consider gauche rotations. A gauche rotation is performed at the randomly choosen bond according to the transition probabilities P_{ij} between state i and j determined by the asymetrical importance sampling technique by Wood (30), and consistent with the rotational-isomerical model. Algebrically the transition probabilities can be written as

$$P_{ij} = \begin{cases} 1/Z & j \neq i \text{ and } u_j \geq u_i \\ u_i/u_j Z & j \neq i \text{ and } u_j \leq u_i \end{cases} \tag{7}$$

$$P_{ii} = 1 - \Sigma P_{ij}$$

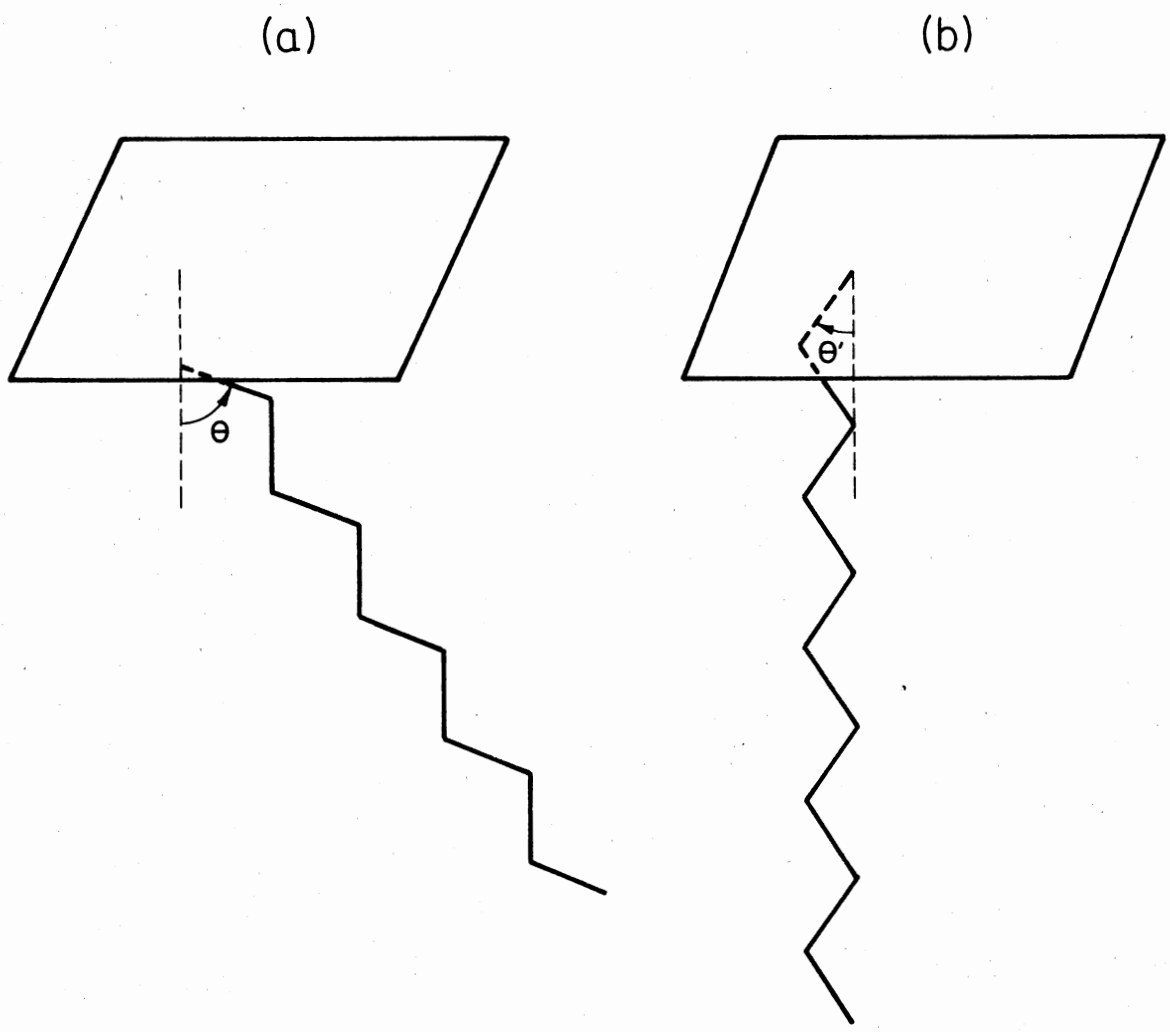

Figure 5. Hydrocarbon Chain Simulated by Monte Carlo Method in Trans State. a) The Hydrocarbon Chain is 35.25° Tilted from X-Axis, Where θ is 70.5°. b) The Hydrocarbon Chain is Perpendicular to YZ-Plane, Where θ' is 35.25°

where $u_i \propto e^{-E_i/kT}$

$u_j \propto e^{-E_j/kT}$

Z is the total number of states.

According to Equation (7), the transition probabilities between two states equal to $\frac{1}{3}\exp(-\Delta E/kT)$ when ΔE $(=E_j-E_i)$ is greater than zero and 1/3 when ΔE is less than or equal to zero. The probabilities that the state is not changed is 1-(probabilities of that states are changed).

In our simulation, the energies we have used are

1. From trans state to $\begin{cases} g^{+120^\circ} & \Delta E=500 \text{ cal/mole} \\ g^{-120^\circ} & \Delta E=500 \text{ cal/mole} \end{cases}$

2. From g^{+120° state to $\begin{cases} \text{trans state} & \Delta E=-500\text{cal/mole} \\ g^{-120^\circ} \text{ state} & \Delta E=2200\text{cal/mole} \end{cases}$

3. From g^{-120° state to $\begin{cases} \text{trans state} & \Delta E=-500\text{cal/mole} \\ g^{+120^\circ} \text{ state} & \Delta E=2200\text{cal/mole}. \end{cases}$

So the transition probabilities are

1. Beginning with trans state
$$P_{tg^+} = \frac{1}{3}\exp(-500/1.987T)$$
$$P_{tg^-} = \frac{1}{3}\exp(-500/1.987T)$$
$$P_{tt} = 1 - \frac{2}{3}\exp(-500/1.987T)$$

2. Beginning with g^{+120° state
$$P_{g^+t} = 1/3$$
$$P_{g^+g^-} = \frac{1}{3}\exp(-2200/1.987T)$$
$$P_{g^+g^+} = 1-\frac{1}{3}-\frac{1}{3}\exp(-2200/1.987T)$$

3. Beginning with $g^{-120^{\circ}}$ state $P_{g^-t} = 1/3$

$$P_{g^-g^+} = \frac{1}{3}\exp(-2200/1.987T)$$

$$P_{g^-g^-} = 1-\frac{1}{3}-\frac{1}{3}\exp(-2200/1.987T).$$

We use rotation operator A_i again to perform rotation. In this case ϕ_i is not zero when gauche rotation occurs. However, one problem arose. Since the method starting with rotation operators operating on the displacement vector $\begin{pmatrix}1\\0\\0\end{pmatrix}$ from Equation (5), leads a vector independent of ϕ_i, then the rotation operator A_i will not cause gauche rotations at even numbered bonds in all trans chain links. To avoid this problem, whenever $\begin{pmatrix}1\\0\\0\end{pmatrix}$ is encountered, we use the rotation matrix shown in Equation (8) to rotate the next bond.

$$A_i' = \begin{bmatrix} \mathrm{Cos}\theta & \mathrm{Sin}\theta & 0 \\ \mathrm{Sin}\theta\mathrm{Cos}\phi_i & -\mathrm{Cos}\theta\mathrm{Cos}\phi_i & -\mathrm{Sin}\phi_i \\ \mathrm{Sin}\theta\mathrm{Sin}\phi_i & -\mathrm{Cos}\theta\mathrm{Sin}\phi_i & \mathrm{Cos}\phi_i \end{bmatrix} \quad (8)$$

In addition to gauche rotations, we use B to rotate the whole chain a random angle about the X-axis.

After each computer run, we apply periodic boundary conditions and check for overlaps. If any two carbon atoms come closer than the fixed hard core diameter, they are said to overlap. The hard core diameter is taken to be 0.95 lattice units. If no overlaps occur, the new position of the carbon atoms and the new state are accepted. If overlap occurs, the old positions of the carbon atoms and the old state is considered as a new state, and the process is repeated.

At each step, the average chain length and average order parameter for carbon are calculated. The order parameter are determined by using the equation

$$S_n = \frac{1}{2} \quad <3\mathrm{Cos}^2 V_m - 1> \tag{9}$$

where V_m describes the deviation of the bond number m from the angle it makes with the X-axis in the trans conformation.

The Monte Carlo average is given by (31)

$$<f> \quad = \frac{1}{N} \sum_{i=1}^{N} f_i \tag{10}$$

where f is an observable quantity, N is the number of steps.

As mentioned on page 18 the chain is allowed to move to any point within a square of side length with finite probability. Therefore, after a large enough number of steps it will reach any point inside the boundary region. Thus our process satisfies the ergodic condition that any configuration can be reached from any other configuration in a finite number of steps. Also the transition probabilities we chose can generate a Markov chain. Markov chains have the properties that successive application of transition probabilities P_{ij} can generate configurations with probability proportional to the Boltzmann factor exp(-E/kT) (31,32) after a sufficient number of steps. So Equation (10) will give us right averages if our steps are large enough. Scott found in his paper (27) that after 60,000 steps the computer runs all seem to converge. In this study, we use 100,000 steps, which should be sufficient. Figure 6 shows the flowchart for the computer simulations.

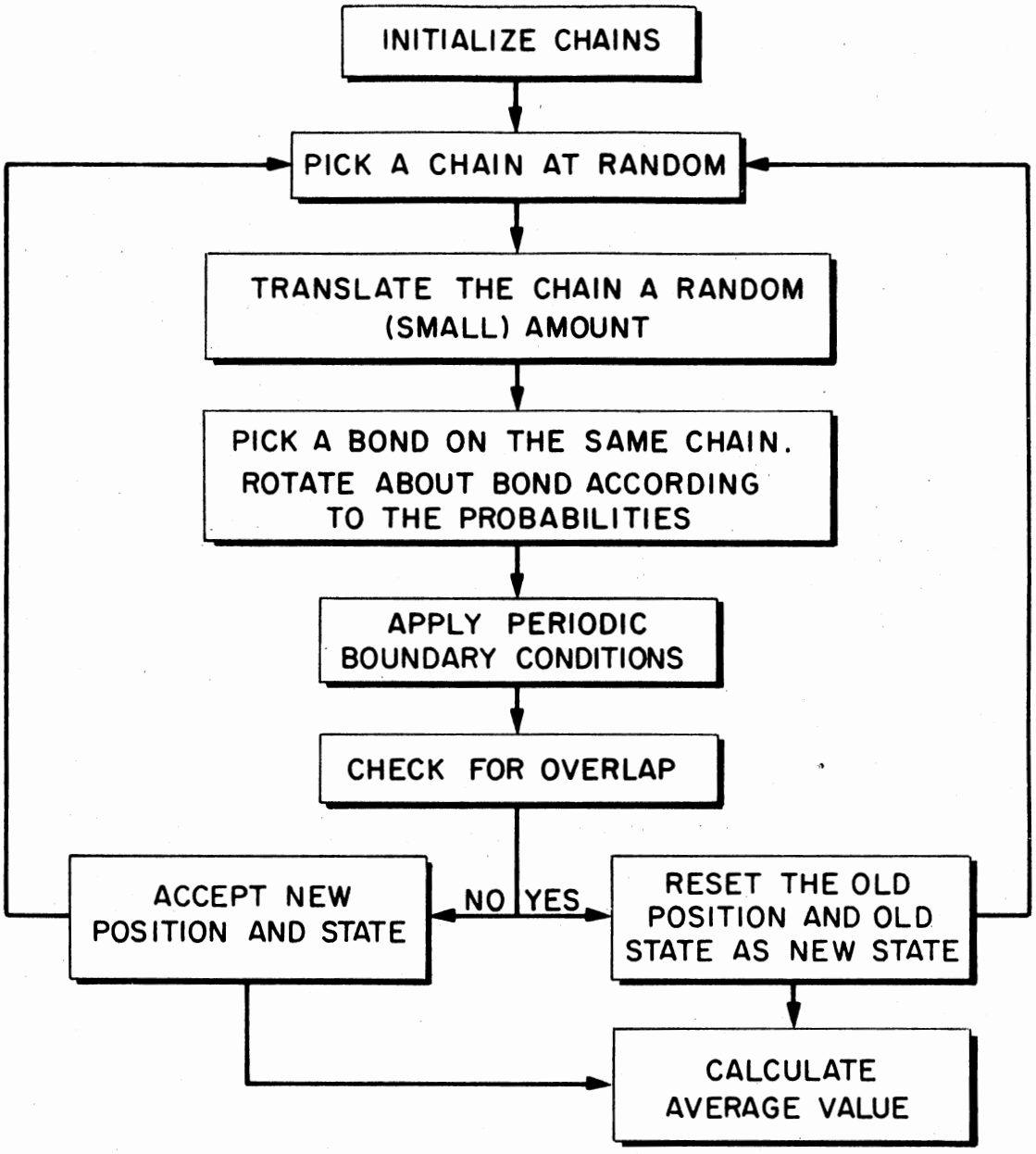

Figure 6. Flow Chart of the Monte Carlo Simulation

We now describe the modifications used in lipid-protein, lipid-cholesterol and curvature bilayer simulations.

Method for Lipid-Protein Interaction

When we initialize the position of lipids, we set the position of protein also. In the present study, a single protein molecule has cylindrical shape with radius of several times the radius of a hydrocarbon chain. The protein is in the center of the confined boundary and penetrates completely through the hydrocarbon chains which are spread out randomly around the protein molecule. We try two runs for two protein radii, 1.5 and 3 times carbon-carbon bond length. We will check the protein size effect on hydrocarbon chain order parameters.

For analyzing boundary lipid, we arranged half of the lipids to locate in a "first nearest neighbor anaulus" around the protein, and the other half to locate in a "second nearest neighbor annulus". In this run, no translational motion of lipids is involved because they are assumed to be bound to the protein molecule. The protein radius for this run was 2.25 times the carbon-carbon bond length. We want to calculate the average chain order parameters for first and second nearest neighbor annuli, and compare these two results.

Method for Lipid-Cholesterol Interaction

The simulation for lipid-cholesterol system is similar to what we did for lipid-protein system, except that we do not let the cholesterol penetrate completely through the lipids and the lipids are allowed

to move laterally. We made two runs with two different penetration depths of cholesterol molecule. The size of the cholesterol molecule we used is two times the carbon-carbon bond length for each run. Again we calculated the order parameters of hydrocarbon chains and compared the differences.

Method for Curved Bilayer

Figure 7 (28) shows part of the lipid bilayer vesicle, where the circles represent head groups and curly line stand for hydrocarbon chains. If we cut the lipid bilayer through AA', then we can see there are two types of curvature. In one, its head group region is narrower than tail region and as shown in Figure 7, in the other its head group region is wider than tail portion. Obviously, the boundaries are not rectangular but trapzoidal in shape. The application of a periodic boundary condition is slightly different from that of a rectangular boundary. If a carbon atom is outside the boundary, as at position P in Figure 13, then we applied periodic boundary conditions to translate this carbon atom to position P' in Figure 13. The details of the application of periodic boundary conditions are shown in the Appendix.

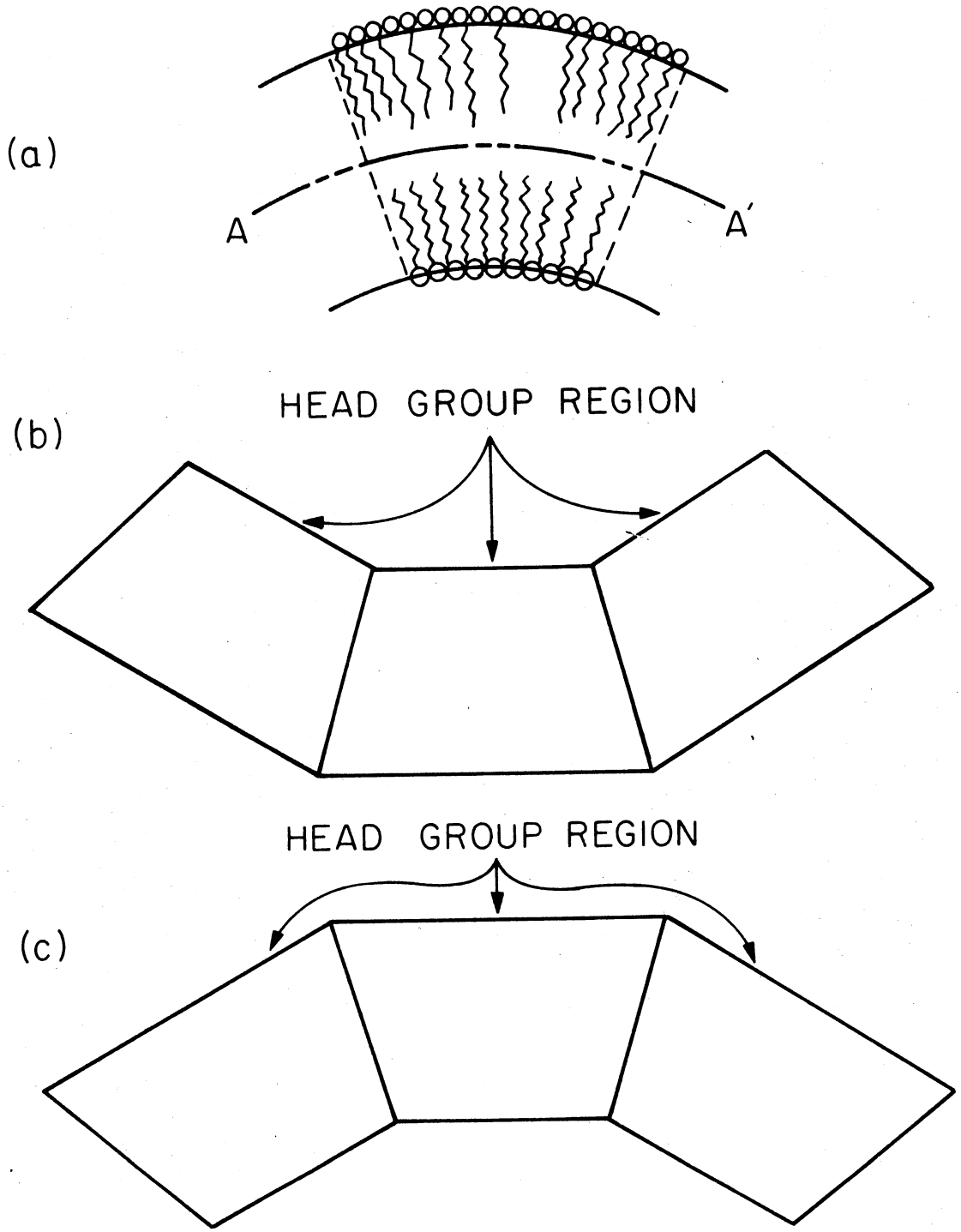

Figure 7. Modified Inner and Outer Monolayers of a Bilayer Vesicle. a) Part of the Vesicle Bilayer. b) Inner Monolayer. c) Outer Monolayer

CHAPTER III

RESULTS AND DISCUSSIONS

Figure 8 through 12 show results of our studies. All figures are plots for a system of eight hydrocarbon chains, each ten links long, confined to different boundary size. In graphs, the boundary size is represented by arrays of various size, in units of bond length, as indicated. The temperature used to determine the rotation probabilities ($\exp(-\Delta E/kT)$) is $300^{o}K$ for all runs. Scott in his earlier paper (27) pointed out that at fixed area, temperature does not sharply affect the order parameter in the hydrocarbon chains. However, varying the molecular area at fixed temperature produced significant changes in the order parameter. It may be argued that when temperature gets higher the area per molecule will increase because of the thermal motion and lateral pressure increased. However, if the pressure of the hydrocarbon is balanced by pressure due to hydrophobic forces in the bilayer, then the area of molecule does not change. Consequently, temperature changes should not produce large scale change in chain ordering. So we only need to try one fixed temperature for all the simulations. All values of order parameters appearing in the figures are Monte Carlo averages after 100,000 steps.

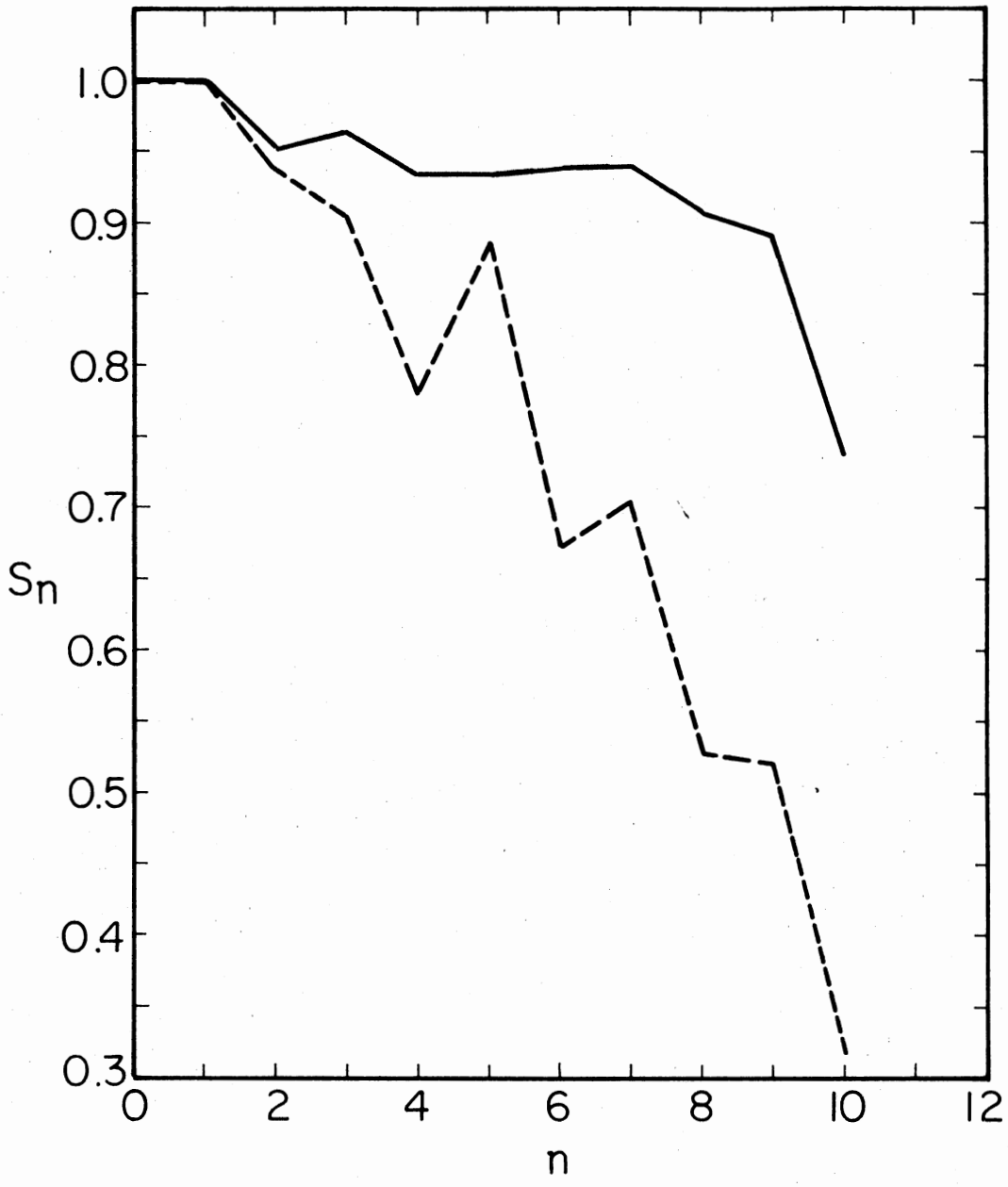

Figure 8. A Plot of Order Parameter Sn vs. Number of Bond n for System of Eight Chains, Each Containing Ten Bonds, and One Protein Molecule with Radii of 1.5 (Represented by Dashed Line) and 3 (Represented by Solid Line) Time C-C Bond Length Respectively

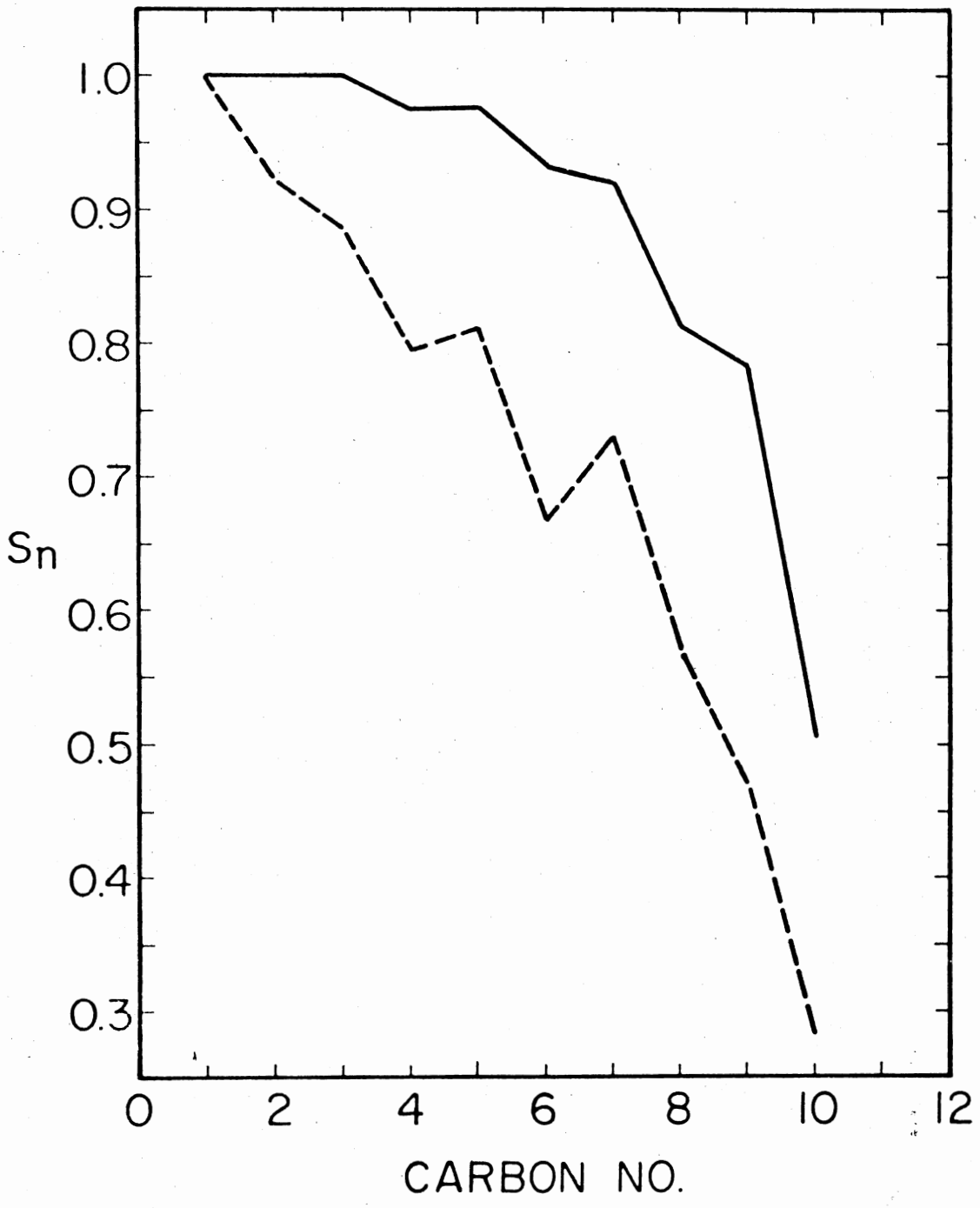

Figure 9. A Plot of Order Parameter Sn vs. Number of Bond n of First (Represented by Solid Line) and Second (Represented by Dashed Line) Nearest Neighbor Annuli for System of Eight Chains, Each Containing Ten Bonds, and One Protein Molecule with Radius of 2.25 Times C-C Bond Length, Confined to 8 x 8 Arrays

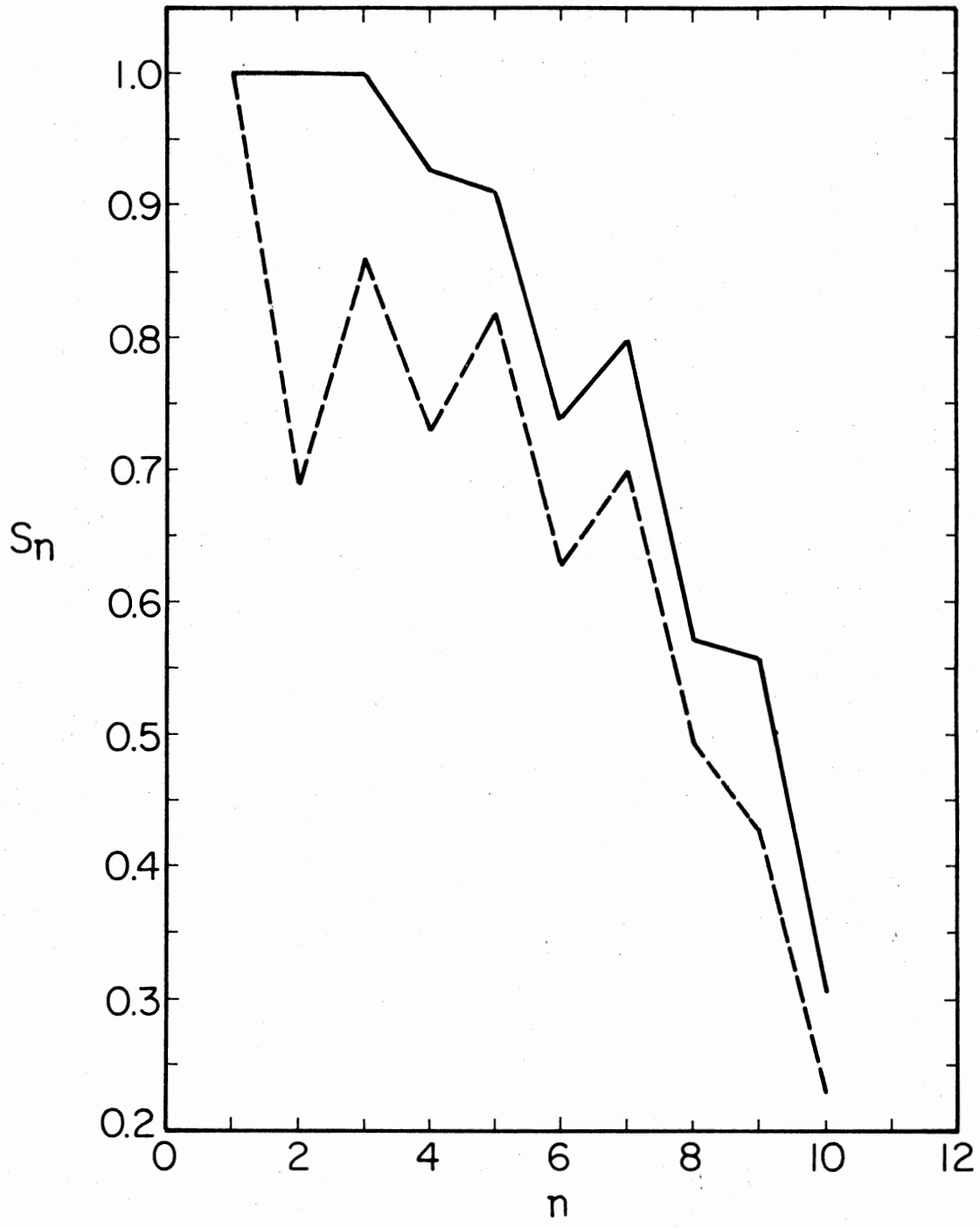

Figure 10. A Plot of Order Parameter Sn vs. Number of Bond n of First (Represented by Solid Line) and Second (Represented by Dashed Line) Nearest Neighbor Annuli for System of Eight Chains, Each Containing Ten Bonds, and One Protein Molecule with Radius of 2.25 Times C-C Bond Length, Confined to 7 x 7 Arrays

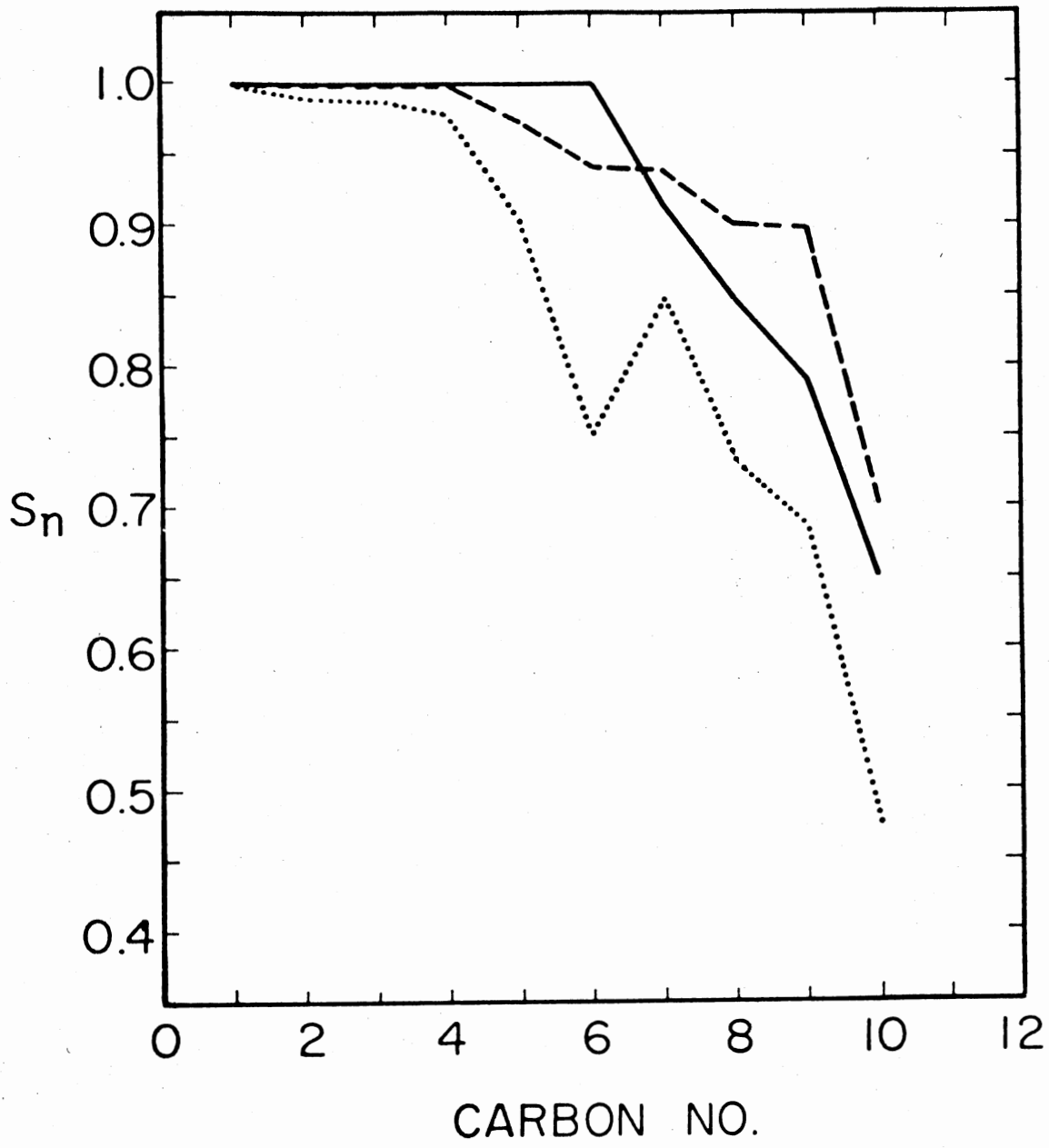

Figure 11. A Plot of Order Parameter Sn vs. Number of Bond n for Systems of Eight Chains, Each Containing Ten Bonds, and One Cholesterol Molecule with Radius 2 Times C-C Bond Length, Confined to 6 x 6 Arrays. The Dotted and Dashed Lines Represented 80% and 35% Penetration of Cholesterol Relative to the Length of an All Trans State Chain

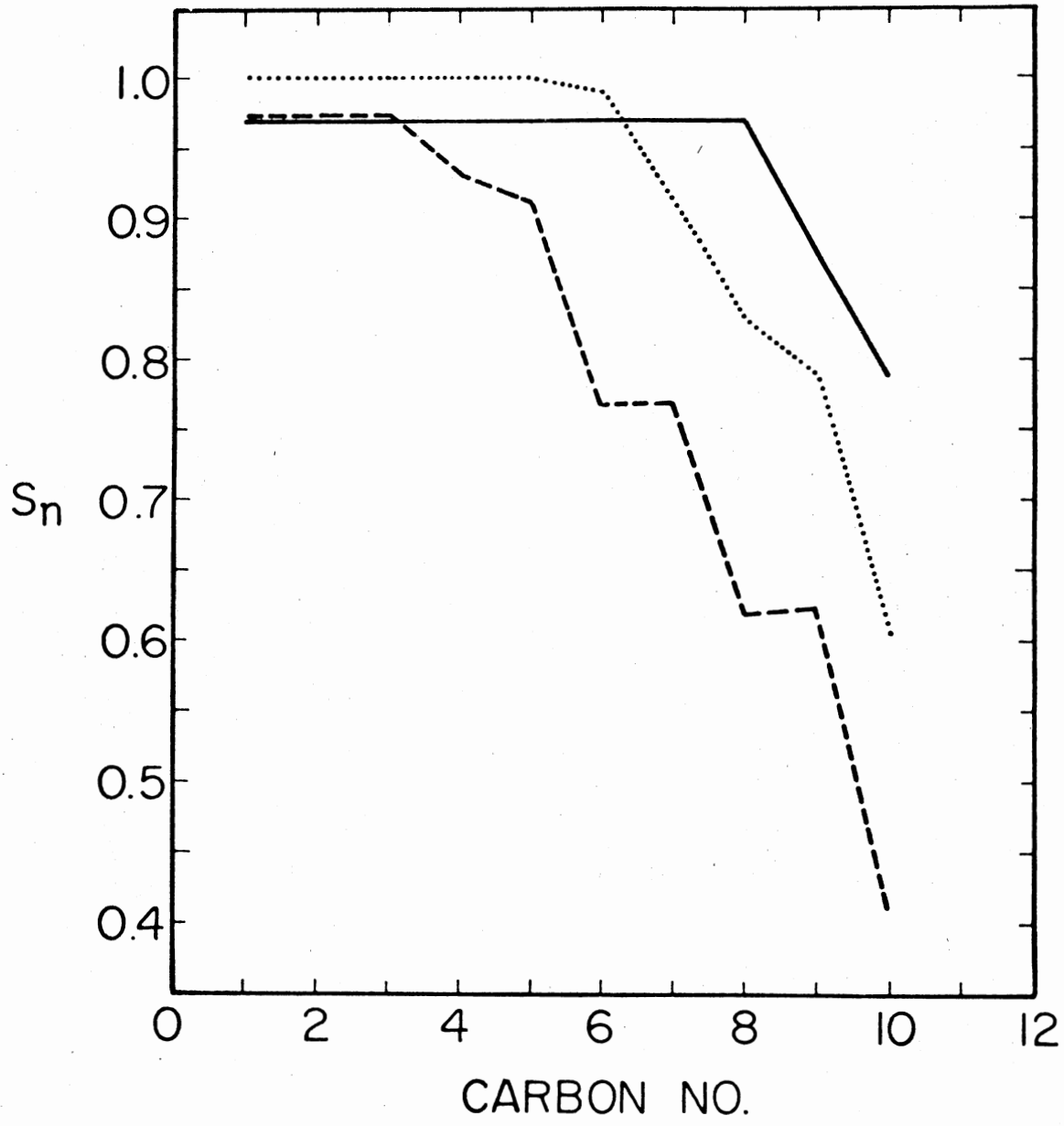

Figure 12. A Plot of Order Parameter Sn vs. Number of Bond n of Inner and Outer Monolayer for Systems of Eight Chains, Each Containing Ten Bonds. For Inner Monolayer (Represented by Solid Line). The System is Confined to 6.5 x 6.5 Arrays (Head Group Region) and 7.5 x 7.5 Arrays (Tail Region). For Outer Monolayer (Represented by Dashed Line), the System is Confined to 5.5 x 5.5 Arrays (Head Group Region) and 4.5 x 4.5 Arrays (Tail Region)

Lipid-Protein Interaction

In Figure 8 we show the effect of protein radii on hydrocarbon chains, by comparing two calculations at two protein radii, 1.5 carbon-carbon bond length and 3 carbon-carbon bond length, for identical systems. Since hydrocarbon chains cannot occupy the volume taken by protein, the larger the protein present the less free volume is available to the hydrocarbon chains. So the hydrocarbon chains remain in a more ordered state. This means that when a protein molecule penetrates a lipid film it will tend to partially immobilize the hydrocarbon chains. This is consistent with the results of protein-monolayer studies (33) which protein interacting with a lipid monolayer increased the surface pressure of the monolayer if all of the protein molecule penetrates through the monolayer.

Figure 9 and Figure 10 represent the Monte Carlo average values of the order parameter S_n for the first and second nearest neighbor annuli of hydrocarbon chains around a protein molecule. The protein radius we simulated for these runs is 2.25 times the carbon-carbon bond length. In Figure 9 the system is confined to 8 x 8 arrays. The order parameters in the first nearest neighbor annulu are greater than in second nearest neighbor annulu. However, the order parameters for first nearest neighbor annulu are not as close to unity as we expected. Probably this is because the system we simulated is not as closely packed as lipids are in bilayers. Such tightly packed systems are not easily simulated by our method as mentioned in Scott's paper (27) since cooperative motions are not allowed. Even so, our results

still show that when protein molecules are present in lipids they will produce different hydrocarbon chain regions, differing markedly in ordering. One region the hydrocarbon chains bound tightly with protein, named boundary lipid. The other region contains more fluid-like lipids.

In Figure 10, the system is confined to 7 x 7 arrays. In contrast with 8 x 8 arrays, the chain density of this system is higher. However, our results are similar to those of Figure 9. This suggests that the amount of lipids bound to the surface of the protein molecule is independent of the extent of the fluid region. It is consistent with spin label results (2,17,18).

Lipid-Cholesterol Interaction

The results of our lipid-cholesterol simulations are shown in Figure 11. The radius of the cholesterol molecule is twice the carbon-carbon bond length. This is close to the real size of the cholesterol molecule. In our simulations we include one cholesterol molecule and eight hydrocarbon chains confined to 6 x 6 arrays. So the molecular ratio of cholesterol to lipid mixture is 1:8 and to hydrocarbon chains only is 1:4.

In reality, the cholesterol molecule is not cylindrical, but the ring region is bigger than the "tail" hydrocarbon chain portion (34). Our model of cholesterol, however, has the same cross-section with a cylindrical shape. We let the cholesterol molecule penetrate the lipid monolayer partially, and see if the penetration depth of the cholesterol molecule effects the order of the hydrocarbon chains. The

results should be qualitatively similar to the system with the real cholesterol molecular shape.

In Figure 11 we show three curves. The dotted and dashed lines represented 80% and 35% penetration relative to the length of an all trans chain. The solid line is the chain order parameters for pure lipid system, included for comparison with the other two curves. As can be seen, the order parameters of dotted and solid line are very close within our method error limits (27). That is because 80% penetration leaves little free volume below the cholesterol molecule for hydrocarbon chain to move. That is why the chains are fairly ordered. However, for 35% penetration shows that the order parameters decrease in the lower part of hydrocarbon chains, corresponding to carbon number n=6 to n=10. This is simply because the free volume below the cholesterol molecule allows the lower region of hydrocarbon chains to have more gauche rotation. The upper part of the chains (about the carbon number from n=1 to n=6) are more ordered and the lower part of the chain (the carbon number from n=6 to n=10) are more fluid. This is consistent with the ESR studies (2), except that their upper part of hydrocarbon chains are more like in all trans state. We did not consider the higher cholesterol concentration like 1:1 to cholesterol:lipid which may exist in some bilayers. For 1:1 cholesterol concentration the upper part of hydrocarbon chains will be more rigid, leaving the lower region still in a more disordered state.

Effects of Bilayer Curvature

In Figure 12 we plot the results of our simulations of bilayer

curvature. The boundary size at outer monolayer we have used are 5.5 x 5.5 arrays for head group region and 4.5 x 4.5 arrays for tail region. For inner monolayer simulation, the arrays of size for head group region is 6.5 x 6.5, increasing to 7.5 x 7.5 in the tail region. Chrezsczyk et al. (28) reported that the area at the inner monolayer varies from 68 $\mathring{A}^2$ at head group to 94 $\mathring{A}^2$ at the tail region and from 74 $\mathring{A}^2$ at head groups to 51 $\mathring{A}^2$ at the tail region in the outer monolayer. The area ratio of head groups to tail region for both inner and outer monolayer are about the same as theirs. The average chain length of our studies is 6.26 carbon-carbon-bond length for inner monolayer and 7.73 carbon-carbon bond length for outer monolayer. Therefore the chain length increases by about 20%. Chrezsczyk et al. (28) found the thickness of inner and outer layer to be 15 $\mathring{A}$ and 20 $\mathring{A}$ respectively. It is about a 25% increase. Comparing our results to theirs, there is some difference between them. It is probably because our system is not as closely packed, or the shape of boundary is different (their system is a truncated pyramid, ours is trapezoid).

As shown in Figure 12, we can see the difference in order parameters of inner and outer monolayers. (The dotted line represents the uncurved lipid system for comparison.) Our results did show the outer monolayer is much more ordered than the inner monolayer. It is the same conclusion drawn from NMR studies by Chrezsczyk et al. (28).

CHAPTER IV

SUMMARY AND SUGGESTIONS FOR FUTURE STUDY

The effects of protein, cholesterol and bilayer curvature on the chain order parameters of lipid monolayer were studied using the Monte Carlo method, extending the method used earlier by Scott (27). For the present studies, we simulated systems consisting of eight chains (each chain containing ten bonds), a protein or cholesterol molecule, confined to a finite size, interacting only via hard core repulsive forces. There are other forces (Van der Waals force) involved in real hydrocarbon chain systems, but our results suggest that the chain order parameters are mainly dependent on the hard core forces. The order parameters did not change significantly when different temperature had been used.

We used different random number generators (changing the order of random number appearing in computer program) to run for identical systems (8 chains, 1 protein, confined to 7 x 7 or 8 x 8 arrays). It was found that the relative difference of Sn were less than 10%. So the shape of the Sn VS. n curve looks the same for all dual runs, up to ~ 10%.

Our results show that the order parameters of hydrocarbon chains depend on the protein size. We simulated the protein molecule as a cylinder in shape. Two radii (1.5 and 3 times C-C bond length) were used. The bigger protein molecule in lipid leaves less free

volume for hydrocarbon chains so the hydrocarbon chains become more stiff. Also our results show that when a protein molecule is present in lipids it will produce a boundary lipid layer around the surface of protein. If the protein molecule extends through the biomembrane, causing a fixed number of lipids to be bound to its surface, it will effectively reduce the number of lipids to form fluid bilayer region in biomembranes. Jost and Marcelja (17,22) reached similar conclusions in experimental and theoretical studies, respectively.

The effect of cholesterol molecule on chain order parameters depend on the penetration depth relative to the all trans length of hydrocarbon chain. For 80% penetration, the chains are rather ordered. That is because 80% penetration saves little free volume below the cholesterol to allow the hydrocarbon chain to move. However, at 35% penetration the presence of cholesterol molecule in lipid tend to decrease the order parameters in the lower part of hydrocarbon chain (carbon atom number n=6 to 10) and increase the order of the upper part of the hydrocarbon chain (n=1 to 6). This is consistent with the results of Kleeman and McConnell's ESR study (2).

We simulated systems with eight chains confined to a trapezoidal bound for a bilayer (monolayer) vesicle. One simulation was with the head group region bigger than the tail region (outer monolayer), the other simulation was with the head group region narrower than tail region (inner monolayer). Our results show that the average chain length is 6.26 times C-C bond length for inner monolayer and is 7.73 times C-C bond length for outer monolayer. So the hydrocarbon chain in outer monolayer is more extended than in inner monolayer.

Since we did not include cooperative motion in our simulations, very closely packed systems are not simulated easily. This is the main short-coming of our Monte Carlo method. However, our results are qualitatively consistent with the experimental conclusions (2,17,18, 22,28) even though we only consider the hard core force.

The present work considered only one protein or cholesterol molecule in lipids. The protein-protein interaction is not included. It is an over-simplified picture compared to the real biomembrane system. When two protein molecules inside the lipids come close to each other, the lipid annuli between the proteins start to overlap. If the protein-protein may still remain separated by lipid annuli. Otherwise the proteins will come together. When a biomembrane system includes lipids, proteins and cholesterol the structure of the membrane is designed to exclude direct interaction of cholesterol with the protein (35). This exclusion is caused by the boundary lipid bound relatively tightly to the protein. So for future studies, we may want to include the cooperative motion in our simulation and consider the systems which have more than one protein molecule and systems with both protein and cholesterol molecules in lipids.

SELECTED BIBLIOGRAPHY

(1) Singer, S. J. and Nicolson, G. L., Science, 175, 720 (1972).

(2) Kleemann, W. and McConnell, H. M., Biochim. Biophys. acta, 419, 206 (1976).

(3) Fox, C. F., Fed. Proc., 30, 1032 (1971).

(4) Kimelberg, H. K. and Papahadjououlos, D., Biochim. Biophys. Acta, 282, 277 (1972).

(5) Harrison, R. and Lunt, G. G., Biological Membranes (a Halsted Press, John Wiley and Sons, Inc., 1975).

(6) Chapman, D., Williams, R. M. and Ladbrooke, B. D., Chem. Phys. Lipid 1, 455 (1967).

(7) Engelman, D. M., J. Mol. Biol., 58, 153 (1971).

(8) Hubbell, W. L. and McConnell, H. M., J. Amer. Chem. Soc., 93, 314 (1971).

(9) Nagle, J. F. and Wilkinson, D. A., Biophys. J. (to be published).

(10) Nagle, J. F., J. Chem. Phys., 58, 252 (1973).

(11) Scott, H. L., J. Chem. Phys., 62, 1347 (1975).

(12) Marcelja, S., Biochim. Biophys. Acta, 367, 165 (1974).

(13) Jacobs, R. E., Hudson, B. and Andersen, H. C., Proc. Nat. Acad. Sci. (U.S.A.), 72, 3993 (1975).

(14) Phillips, M. C. and Chapman, D., Biochim. Biophys. Acta, 163, 301 (1968).

(15) Vail, W. J., Papahadjopoulos, D. and Moscarello, M. A., Biochim. Biophys. Acta, 345, 463 (1974).

(16) Engelman, D. M. and Rothman, J. E., J. Biol. Chem., 247, 3694 (1972).

(17) Jost, P., Griffith, O. H., Capaldi, R. A. and Vanderkooi, G., Biochim. Biophys. Acta, 311, 141 (1973).

(18) Jost, P., Griffith, O. H., Capaldi, R. A. and Vanderkooi, G., Proc. Natl. Acad. Sci. U.S.A. 70, 480 (1973).

(19) Chapman, D., Urbina, J. and Keough, K. M., J. Biol. Chem., 249, 2512 (1974).

(20) Papahadjopoulos, D., Moscarello, M., Eylar, E. H. and Isac, T., Biochim. Biophys. Acta, 401, 317 (1975).

(21) Kimelberg, H. K. and Papahadjopoulos, D., Biochim. Biophys. Acta, 233, 805 (1971).

(22) Marcelja, S., Biochim. Biophys. Acta, 455, 1 (1976).

(23) Chapman, D. and Penkett, S. A., Nature, 211, 1304 (1966).

(24) Lecuyer, H. and Dervichian, D. G., J. Mol. Biol., 45, 39 (1969).

(25) Ladbrooke, B. D., Williams, R. M. and Chapman, D., Biochim. Biophys. Acta, 150, 333 (1968).

(26) Papahadjopoulos, D., Nir, S. and Ohki, S., Biochim. Biophys. Acta, 266, 561 (1971).

(27) Scott, H. L., Biochim. Biophys. Acta, 469, 264 (1977).

(28) Chrzeszczyk, A., Wishnia, A. and Springer, C. S., Biochim. Biophys. Acta, 470, 161 (1977).

(29) Hammersley, J. M. and Handscomb, D. C., Monte Carlo Methods (Methuen London, 1964).

(30) Wood, W. W., Physics of Simple Liquids, (Temperley, H. V. V., Rowlinson, J. S. and Rushbrooke, G. S., eds.) Wiley Interscience, New York.

(31) Metropolis, N., Rosenbluth, A. W., Rosenbluth, M. N., Teller, A. H. and Teller, E., J. Chem. Phys., 21, 1087 (1953).

(32) Wood, W. W. and Parker, F. R., J. Chem. Phys., 27, 720 (1957).

(33) Shafter, P. T., Biochim. Biophys. Acta, 373, 425 (1974).

(34) Rothman, J. E. and Engelman, D. M., Nature New Biology, 237, 42 (1972).

(35) Warren, G. B., Houslay, M. D., Metcalfe, J. C. and Birdsall, N. J. M., Nature, 255, 684 (1975).

APPENDIX

APPLICATION OF PERIODIC BOUNDARY CONDITION FOR CURVATURE LIPID BILAYER

In Figure 13, the trapezoid ABCD is chosen as a reference trapezoid. The height of this trapezoid we used is the same as the length of hydrocarbon chains in all trans state. For ten bond hydrocarbon chain, the length is 8.1664095 times carbon-carbon bond length. If any carbon atom P of any chain is outside the trapezoid ABCD, we can use the data we know to translate the coordinates of carbon atom P to P' in reference trapezoid ABCD. In Figure 13a, the head group is on the top (confined to 4.5 x 4.5 arrays) and the tail region is on the bottom (confined to 5.5 x 5.5 arrays). The coordinates of carbon atom P shown in Figure 13a is (QP,RP) in XY-plane. From Figure 13a, we can see AE is 8.1664095 (the height of the trapezoid), AR = DE - QP, and the angles are

$$m < DAE = \tan^{-1} \frac{DE}{AE}$$

$$m < SAR = m < DAE$$

$$m < RAP = \tan^{-1} \frac{AR}{RP}$$

$$m < SAP = m < SAR + m < RAP$$

the length of AP is

$$AP = (AR^2 + RP^2)^{1/2}$$

then we can figure out the length of AS and PS shown in Figure 13a.

$$AS = AP \cdot \mathrm{Cos}(m < SAP)$$

$$PS = AP \cdot \mathrm{Sin}(m < SAP)$$

Now we take BS' = AS and P'S' + PS, so the coordinates of carbon atom become (P'S', D'B - S'B) at point P'.

Figure 13b represents the outer monolayer, the head group is confined to 5.5 x 5.5 arrays and the tail region is confined to 4.5 x 4.5

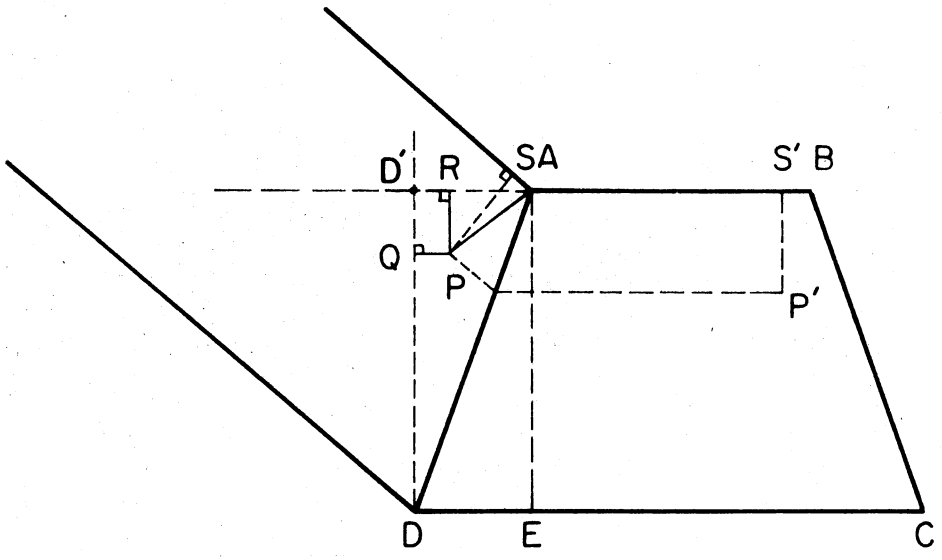

(a)

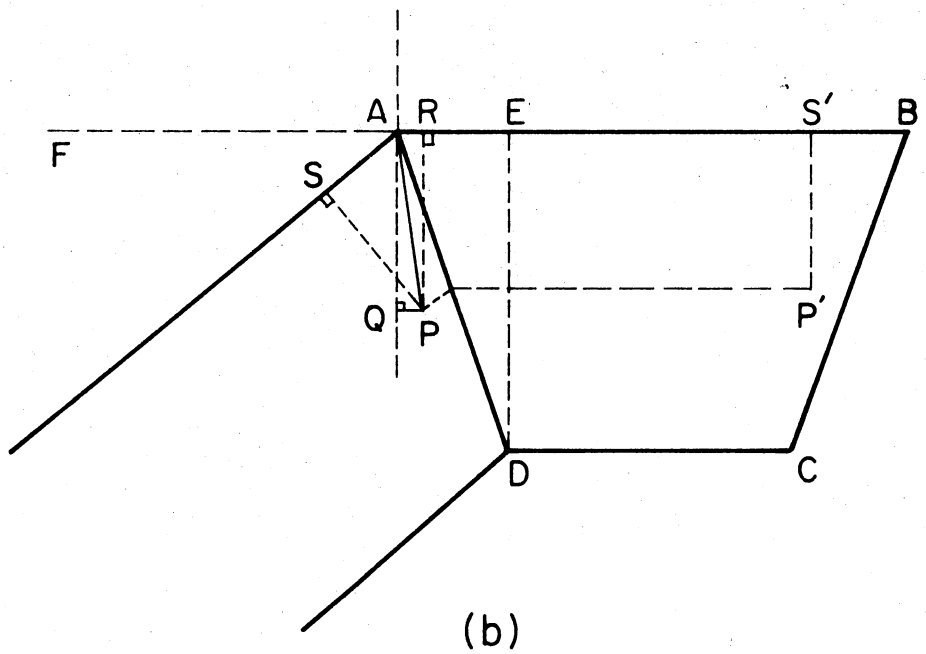

(b)

Figure 13. A Diagram Showing How the Periodic Boundary Conditions Were Applied. a) Inner Monolayer, b) Outer Monolayer

arrays. The procedure is about the same as the inner monolayer case. As shown in Figure 13b, DE = 8.1664095, the angles are

$$m < FAS = 2 \tan^{-1} \frac{AE}{ED}$$

$$m < SAQ = \frac{\pi}{2} - m < FAS$$

$$m < SAP = m < SAQ + m < QAP$$

the length of AP is

$$AP = (PQ^2 + AQ^2)^{1/2}$$

where PQ, AQ are the coordinates projected on X and Y axes. Then we can calculate the length of AS and PS

$$AS = AP \cdot \mathrm{Cos}(m < SAP)$$

$$PS = AP \cdot \mathrm{Sin}(m < SAP)$$

We set BS' = AS and P'S' = PS, so the coordinates of carbon P now become (S'P', AB-BS') at point P'.

VITA[2]

Sheau-Lin Sharon Cherng

Candidate for the Degree of

Master of Science

Thesis: MONTE CARLO STUDIES OF THE EFFECTS OF PROTEIN, CHOLESTEROL AND CURVATURE ON LIPID ORDER PARAMETERS

Major Field: Physics

Biographical:

Personal: Born in Kaohsiung, Taiwan, Republic of China, March 23, 1951, the daughter of Pang-Feng and Ju-Ching Cherng.

Education: Graduated from Kaohsiung Girls High School in Kaohsiung, Taiwan, Republic of China, in June, 1968; received Bachelor of Science degree in Physics from National Taiwan Normal University in Taipei, Taiwan, Republic of China in June, 1973; completed requirements for Master of Science degree at Oklahoma State University in May, 1978.